Reprocessable Polyurethane Foams using Acetoacetyl Formed Amides

*Hiba Kassem[1,2], Lucie Imbernon[2], Lucas Stricker[1], Laura Jonckheere[2], Filip E. Du Prez[1]**

[1]Polymer Chemistry Research Group, Centre of Macromolecular Chemistry (CMaC),
Department of Organic and Macromolecular Chemistry, Faculty of Sciences, Ghent University,
Krijgslaan 281 S4-bis, 9000 Ghent, Belgium.

[2]Recticel NV, Damstraat 2, Industriezone 7, 9230 Wetteren, Belgium.

E-mail: Filip.DuPrez@UGent.be

KEYWORDS

Polyurethane foams, dynamic materials, reprocessability, amides, polyurethane

ABSTRACT

Like any other thermosetting material, polyurethane foams (PUFs) contain permanent crosslinks that hinder their reprocessability and make their recyclability a tedious and environmentally unfriendly process. Herein, we introduce acetoacetyl formed amides, formed by the reaction of isocyanates with acetoacetate groups, as dynamic units in the backbone of PUFs. By extensive variation of the foam composition, optimum parameters have been found to produce malleable foams above temperatures of 130 °C, without the requirement of any solvent during the foaming process. The PU crosslinked material can be compression molded at least three times, giving rise to PU-elastomers and thus maintaining a crosslinked network structure. Characterization of the original foams shows comparable properties to standard PUFs, for example having a density of 32 kg/m^3, while they show similar chemical and thermal properties upon reprocessing to strong PU-elastomers, exhibiting a T_g ranging from -42 to -48 °C. This research provides a straightforward method to produce thermally reprocessable PUFs as a promising pathway to address the recycling issues of end-of-life foams.

INTRODUCTION

The unique physical, mechanical and insulation properties of polyurethanes (PUs) are the main drivers for their increasing market share.[1] Owing to these features, PUs are currently versatile materials used under many different forms (e.g., coatings, elastomers, foams) in a broad range of applications (e.g., bedding, automotive, insulation).[2] The simultaneous high production and consumption of PUs generate a significant volume of accumulated waste.[3] A quite significant portion of this waste (60% in Europe) corresponds to polyurethane foams (PUFs) due to their low densities[4,5]. Like other thermosetting materials, PUFs can either be mechanically recycled after which they are used as fillers or rebounded into new denser materials, or chemically recycled to polyols and other chemical compounds via chemical recycling.[3,6–13] These recycling methods suffer from significant disadvantages, such as poor quality of the mechanically recycled products or often tedious purification techniques that are required for chemical recycling.[3]

In 2010, the concept of covalent adaptable networks (CANs) was introduced to the scientific community by Bowman and Kloxin.[14–16] Unlike traditional thermosets, CANs can be reshaped or repaired under certain external stimuli (e.g., heat, light) owing to the presence of reversible or exchangeable bonds.[17,18] CANs are classified into associative or dissociative types according to the dynamic chemistry used.[18,19] Associative CANs make use of dynamic chemistries for which the bond-breaking and bond-making processes happen simultaneously (e.g., S_N2 reactions), leading to a constant cross-link density over different processing temperatures.[20,21] On the other hand, dissociative CANs contain dynamic chemistries for which those two processes are happening in a consecutive way (e.g., Diels-Alder reactions).[22,23] Numerous dynamic chemistries have been investigated to prepare CANs such as disulfides, siloxanes, vinylogous urethanes and many more.[24,25,34–43,26,44,45,27–33]

Transcarbamoylation has previously been investigated as a way to introduce dynamic behavior in PUFs.[46,47] Sheppard and coworkers soaked PUF into a dibutyltin dilaureate (DBTL) solution, evaporated the solvent, and reprocessed lab-made and post-consumer PUFs at elevated temperatures.[48] Indeed, the DBTL catalyst triggered the transcarbamoylation reaction in the foams, making them extrudable.[48] However, this solvent processing technique is neither scalable nor environmentally friendly due to the use of high amounts of a tin catalyst (up to 0.3g of DBTL for 1g of foam). Wang and coworkers alleviated this issue by applying a disulfide-based cross-linker for the PUF-design.[49] They synthesized malleable and thermally recyclable polyurethane/ polythiourethane foams directly via the incorporation of raw materials containing covalent adaptable bonds. Their foams are shown to be recyclable as a result of the disulfide exchanges at elevated temperatures (around 180 °C)[49]. However, the quite elevated temperature used to reshape the foams is not favorable because this is expected to result in side reactions, for example with remaining water present in the foam, affecting its hydrolytic stability. Finally, a few studies have focused on the fabrication of a CAN that was foamed in a second step using supercritical CO_2.

However, this method has economical drawbacks, and the produced foams generally possess reduced properties compared to standard PUFs. [50–54]

Acetoacetates are bulk chemical compounds, used in paint industry, for example, that can form vinylogous urethanes when reacted with amines.[29] Earlier, we demonstrated that those vinylogous urethanes can become themselves dynamic in the presence of free amines.[30] On the other hand, already in 1979, the reaction between an acetoacetate and isocyanate was reported.[55] Since then, acetoacetates have been used widely in combination with isocyanates to form acetoacetyl formed amides (AFAs) (Scheme 1a).[56–58] While AFAs have been exploited in the coating industry, it was only in 2019 that Shi and coworkers reported that AFAs possess a dynamic behavior at elevated temperature (> 160°C), giving rise to a ketene and an amine as intermediate compounds (Scheme 1b)[59].

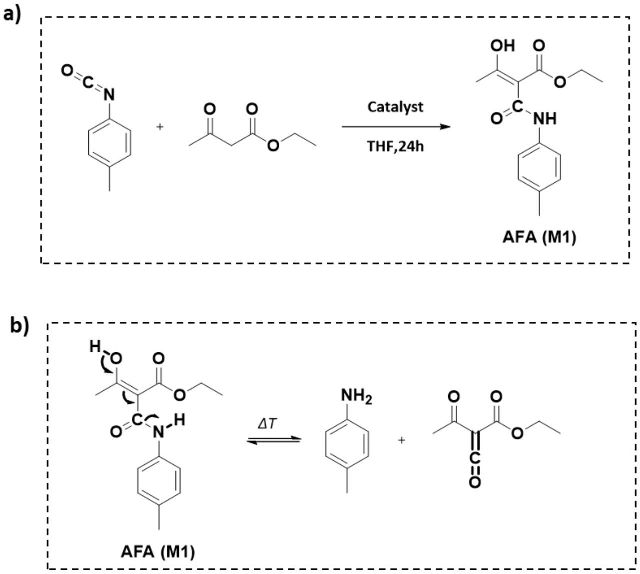

Scheme 1. (a) Reaction between p-tolyl isocyanate and ethyl acetoacetate, leading to the AFA model molecule M1. (b) dissociative reaction mechanism of M1 at elevated temperature to p-toluidine and a ketene-containing compound (ketene function shown in bold).

In 2021, they further investigated a multiple component reaction taking place between acetoacetate, isocyanate and amines, leading at elevated temperatures to an adduct that produces a vinylogous urethane and an isocyanate as an intermediate.[60,61]

Producing stable and high performance PUFs is based on optimized industrial processes that can be influenced by a multitude of reaction parameters including catalysis, stabilizers, additives and blowing agents. In other words, the incorporation of a new type of dynamic bond into such foams can be a highly challenging task. In view of the high societal need for more sustainable routes to recycle polyurethane foams, we therefore envisaged exploring the AFA dynamic chemistry in standard PUF-formulations, using a straightforward and scalable approach. In first instance, an appropriate catalyst for the AFA formation had to be found in order to adapt the reaction rate to the PU foaming process. A screening of different catalysts was thus performed in a model study. For a better understanding of the dynamic character of the AFA-based networks and before the preparation of PUFs using a standard foaming technique, hybrid PU-elastomers containing AFA as well as urethane bonds were studied. Furthermore, it will be shown that the obtained foams can be reprocessed using compression molding to high-quality elastomers that in turn can also be reprocessed at least two times at relatively low temperatures (> 130°C) without the use of any solvents. The full characterization of both the PUFs and the corresponding elastomers will be discussed.

RESULTS AND DISCUSSION

As the primary aim of this work was to introduce the AFA-bonds in standard PUF as thermally triggered dynamic bonds, we investigated the thermally activated dynamic exchange in detail. For this, AFA-containing model molecules M1, M2, and M3 (Figure 1a, Figures S1-S3) were synthesized according to an available protocol[59].

M1 was dissolved in THF at room temperature, after which it was gradually heated to 100 °C and cooled again while following the dissociation with online-FTIR. The height of the stretching ketene peak (C=C=O) at 2145 cm^{-1} was followed and recorded over time (Scheme 1b, Figure 1b).

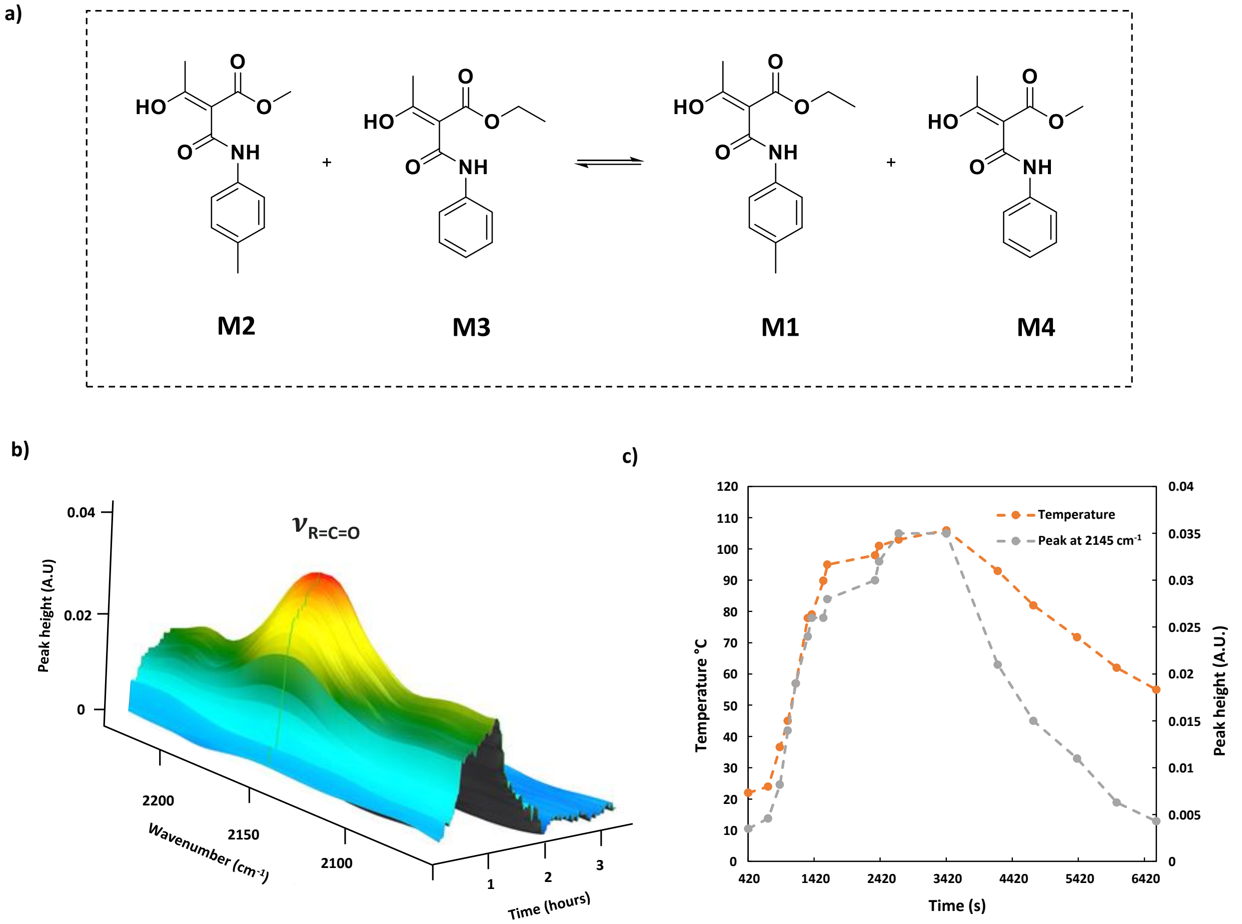

Figure 1. (a) reaction scheme between M2 and M3 (b) waterfall plot showing the increase in the peak height of the ketene function (2145 cm^{-1}) and its decrease over time, (c) the normalized change in the peak height of ketene C=C=O stretching (2145 cm^{-1}) with corresponding temperature.

The resulting FTIR-spectra confirmed that M1 indeed dissociates with increasing temperature, giving rise to a ketene and a primary amine (latter not shown). The ketene peak gradually disappears upon cooling to room temperature (Figure 1c), confirming the reversibility of such an AFA moiety. To further investigate the exchange reaction with these molecules, the exchange between M2 and M3 was examined by liquid chromatography-mass spectrometry (LC-MS) (Figure S4). For this, M2 and M3 were mixed in acetonitrile under nitrogen flow and subsequently heated to 80 °C. The LC-MS peaks assigned to M2 and M3 broaden and new peaks belonging to M1 and a new molecule that we attribute as M4 are observed (Figure S5), thus again confirming the exchange.

Following a literature report, the model molecules (M1-M3) were initially synthesized using Et_3N as a catalyst.[59] However, the reaction time required for full conversion was relatively long (> 24h) and would not be suitable at all for the standard PU foaming process. For this reason, a kinetic study was carried out with a series of catalysts (DBU, DABCO, P-TSA, Niax A133, TBD, ET_3N, DMEA, and DBTL) (Figures S6-13). For this, 0.72 mmol of catalyst was used in all cases. Online-FTIR was employed to monitor on the one hand the disappearance of the stretching isocyanate peak (N=C=O) at 2273 cm^{-1} and on the other hand the formation of the stretching peak of the secondary amide (C=O) ranging between 1470 to 1570 cm^{-1}.[62,63] Based on this catalyst screening (Table S1), DBU was shown to be the most efficient catalyst for AFA bond formation, as the full reaction of the isocyanate with the acetoacetate is achieved in only 3h in presence of this catalyst (Figure S6). DBU was therefore used in the upcoming material synthesis. Scheme 2 shows a plausible reaction mechanism in which DBU acts as a strong base and deprotonates the alpha carbon of the acetoacetate, while the resulting anion reacts as a nucleophile with the isocyanate group.

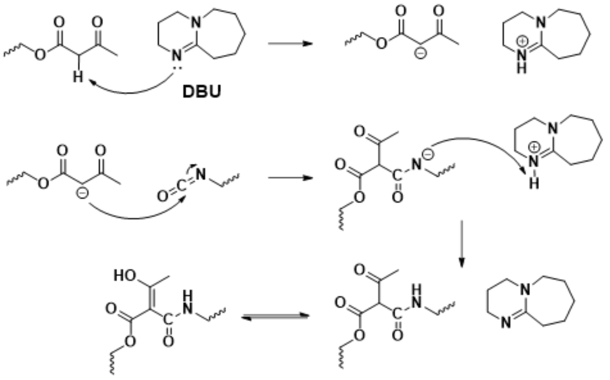

Scheme 2. Proposed pathway for the DBU-catalyzed formation of an acetoacetyl formed amide.

To prove the dynamic behavior of AFA chemistry on material level before its introduction in foams, two AFA-based elastomeric CANs were synthesized (Table 1). For this, a hydrophobic terpene-based polyol (Pripol 2043) was selected as the starting compound for both elastomers. To introduce the acetoacetate functionality, this polyol was first acetoacetylated via a condensation reaction using tert-butyl acetoacetate according to an earlier reported and scalable procedure (Figure S14-17).[41] To have a benchmark AFA-network, an elastomer containing only AFA matrix, i.e. using only acetoacetylated Pripol 2043, was synthesized by combining it with toluene diisocyanate and DBU as catalyst (AFA1). Then, importantly, to check if this chemistry is compatible when introduced in a urethane containing matrix, an elastomer containing 14 mol% of Caradol SC 48-08, which is an industrially used propylene oxide/ethylene oxide-based polyether polyol, 86 mol% of acetoacetylated Pripol 2043, toluene diisocyanate, DBU and DBTL was also prepared (AFA2). Both samples were cured in the oven at 60 °C for 24h before they were reprocessed. The initial elastomers and their reprocessed samples (after each consecutive reprocessing step) were characterized. Solubility tests and thermal characterization on both AFA-based networks showed similar solubility fractions, swelling ratios and glass transition temperatures (Table 1).

Table 1. Overview of composition and physical properties of the two AFA-based elastomers.

CAN	AFA bonds [mol%]	Urethane bonds [mol%]	T_g [a] [°C]	$T_{d5\%}$ [b] [°C]	Swel. Rat. [c] [wt%]	Sol. Frac. [c] [wt%]	$\tau_{110°C}$ [e] [s]	E_a [f] [KJ/mol]
AFA1	100	0	13	261	312 ± 2	9.1±0.4	134	217±14
AFA2	86	14	18	266	360 ± 5	6.1±1.1	279	266 ±27

[a] Determined from the second heating (½ ΔCp) in DSC analysis (10 °C.min^{-1}); [b] TGA onset temperatures after 5% weight loss ($T_{d5\%}$); [c] swelling ratio and solubility fraction in THF obtained from three sample measurement at r.t. for 24h; [e] characteristic relaxation time (τ) at 110 °C obtained from stress relaxation experiments; [f] activation energy (E_a) obtained from Arrhenius plot.

To explore the reprocessability of these CANs, the samples were cut into pieces and compression molded to a one-piece material at 110 °C under a pressure of 4 tons (Figure 2). The reprocessing temperature was selected in order to stay well below the transcarbamoylation exchange temperature (>150°C).[64,65] This reprocessing cycle could be repeated at least three times; the corresponding materials are further referred to as AFA_Rx (where x indicates the number of the reprocessing cycle).

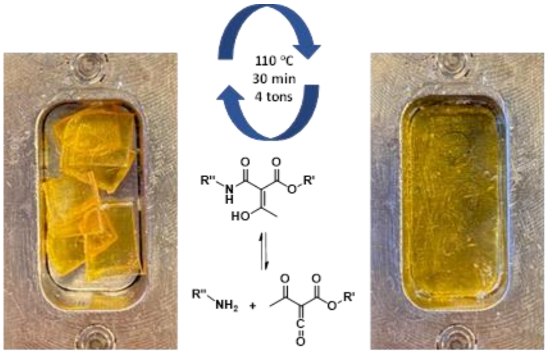

Figure 2. Visualization of the reprocessed elastomeric sample AFA1 via compression molding at 110°C (4 tons for 30 minutes).

Stress relaxation experiments have been performed on AFA1_R1 and AFA2_R1 to investigate the dynamic properties of the CANs. The stress relaxation temperatures were analyzed as a function of temperature according to the stretched Maxwell model, where the relaxation time was calculated according to Equation S3 (Figure 3).

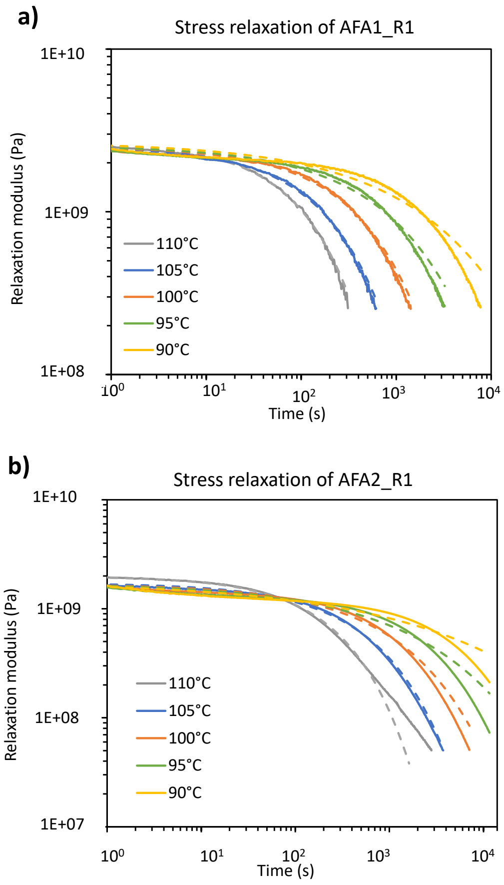

Figure 3. Non-normalized stress–relaxation plots of AFA1_R1 (a), AFA2_R1 (b) from 110 to 90°C; the fitting with a stretched Maxwell model given in dashed lines.

As a result of bubble formation above 115°C, which is ascribed to trapped tert-butyl acetoacetate and/or tert-butyl alcohol, those stress relaxation measurements were limited to a small temperature window. Notably, a faster stress relaxation time that is interpreted as a higher exchange rate, was observed for AFA1 (τ= 134 s) compared to AFA2 (τ= 297 s) at 110 °C. This can be ascribed to the presence of permanent urethane bonds at 110 °C in AFA2, which makes the exchange rate slower. At higher temperatures, the deviation from the Arrhenius plot is attributed to the presence of these urethane bonds that start to show dynamicity, adding a second overlaying dynamic exchange reaction to the stress relaxation.[66] On the other hand, the dynamic behavior of PU-bonds can also lead to irreversible side reactions, which may cause the deviation from the Arrhenius plot at lower temperatures (Figure 3). Moreover, FTIR analysis confirms that upon CAN-reprocessing no significant changes in the chemical structure occur (Figure S18-20) and the thermal properties of the reprocessed samples do not show major differences upon recycling (Figure S21-22).

After confirming the thermally activated exchange of AFA bonds and their compatibility with the PU-matrix, the next step was to explore the introduction of those dynamic bonds into PUFs. Towards this goal, PUF that are containing AFA networks were prepared using a standard batch foaming procedure that is further described in the SI. A wide range of foams were prepared using variable amounts of AFA bonds (between 26 and 92 mol%, not listed in Table 2). As a result of this screening, we concluded that the minimum amount of AFA that is required to make a reprocessable AFA-based foam is 86 mol% (Table S3) while AFA amounts exceeding 89 mol% resulted in the collapse of the foam (Figure S34). Based on those first results, three foams containing 86 mol% of AFA bonds were synthesized with variable DBU and DBTL content, while maintaining the amounts of the other components stable (Table 2).

The foam samples are further referred to as AFAFx in which x is the foam number. As a benchmark material, a standard PUF was also synthesized.

Table 2. AFA-based foam (AFAF) catalyst composition and their corresponding physical properties.

Foam[a]	DBTL wt%	DBU wt%	density[b] kg/m^3	Comp.[c] %	Tensile Strength[d] kPa	Elongation[e] %	Tear resistance[f] N/cm	Cell size[g] mm	T_g[h] °C	$T_{d5\%}$[i] °C
PUF	0.4	0	32.3	2	83±11	102±17	2.2	1.2	-55	276
AFA F1	1.65	0.65	33.1	47.3	38±6	60±12	1.6	1.6	-48	244
AFA F2	0.8	0.5	32.1	49.2	41±6	58±6	1.5	1.2	-42	240
AFA F3	0.8	0.3	32.1	49.2	17±9	40±18	1.4	1.2	-42	249

a)PUF contains 100 mol% of urethane bonds and AFAF1, 2 and 3 contain 14 mol% of urethane bonds and 86 mol% of AFA bonds; b) Calculated average density from four different locations on the foam; c) compression set was calculated as the average from four sample measurements; d) Tensile strength was calculated as the average of three sample measurements with standard deviation; e) elongation at break were obtained from the average four sample measurements with standard deviation; f) tear resistance values were obtained from the average of three sample measurements; g) cell size was obtained from SEM images; h) Determined from the second heating in DSC analysis (10 °C.min^{-1}); i) TGA onset temperatures after 5% weight loss ($T_{d5\%}$)

During the PU foaming process, two main reactions are taking place simultaneously, being the blow and gel reactions. On the one hand, in the presence of amine catalysts, the blowing reaction happens between isocyanates and water with the production of CO_2. The gel reaction, on the other hand, is a step growth polymerization that occurs between polyol (Caradol SC 48-08 in this case) and isocyanates (here toluene diisocyanate) to form urethane bonds. DBTL is used as catalyst for this reaction, which according to the Bloodworth's mechanism acts as a Lewis acid.[67] The role of DBU is to catalyze the AFA-reaction which was already described in Scheme 2.[68] Furthermore, Niax L620 has been introduced as an organosilicone surfactant, which is usually applied to enhance the cell formation within the foam by increasing the nucleation sites and stabilizing the cells during the blow and gel reactions.

Upon characterization of the synthesized foams, no major differences were observed in the thermal properties (Table 2). The DSC thermograms indicated that the AFAFs displayed T_g values in the range of -48 to -42 °C (Figure S24). Moreover, the thermal degradation of the AFA-based foams also revealed no significant differences as the $T_{d5\%}$ ranged from 240 to 249 °C (Figure S26). Remarkably, the morphological properties such as the foam density and the cell sizes are similar in comparison to the standard PUF exhibiting a density of 32 kg/cm^3 and cell sizes ranging from 1.2 to 1.6 mm. Also, an optical visualization of the cells via SEM-analysis showed a comparable and relatively open-cell structure in all foams, which indicates the character of a typical flexible PUF (Figure 4).

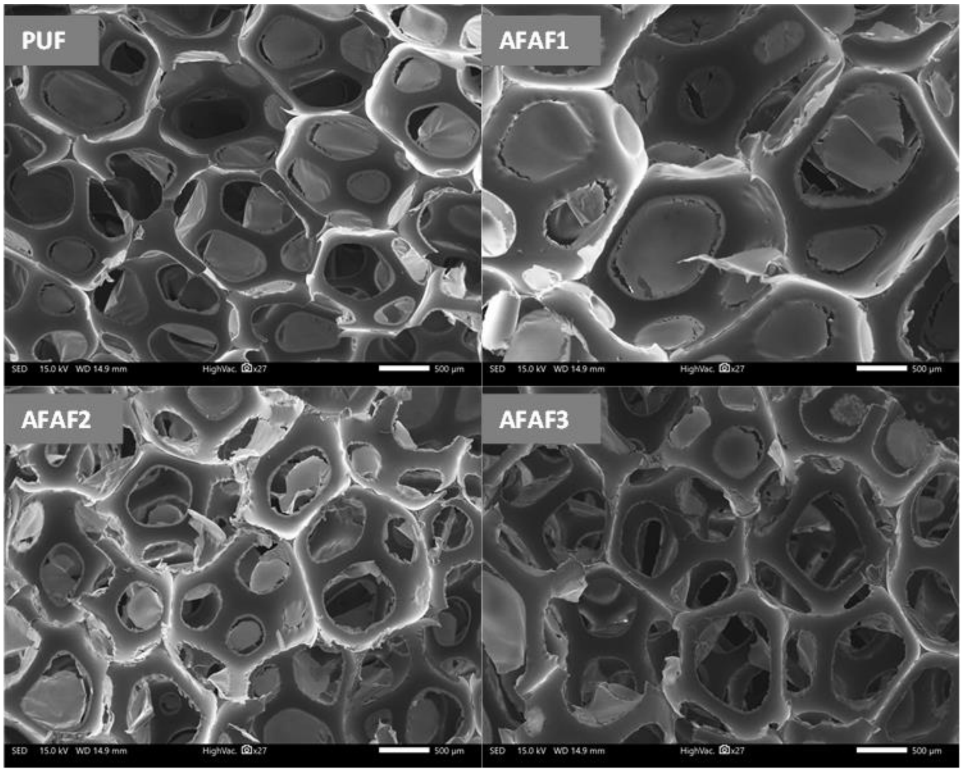

Figure 4. SEM images showing the cell morphology of the benchmark PUF and 3 AFA-containing foam samples (scale bar is 500 μm).

The mechanical properties showed that AFAF3, which contains the lowest amount of DBU (0.3 wt%) amongst all stable foams, exhibited the lowest tensile strength (17±9 kPa), elongation at break (40±18 %) and tear resistance (1.4N/cm) (Figure 5). In comparison to PUFs, AFAFs displayed overall (slightly) weaker mechanical and thermal properties, thus a follow-up optimization study would be necessary to make an industrial implementation of such AFA-PUFs feasible. The AFAFs were cut into pieces and compression molded at 140°C for 30 to 45 minutes (pressure 5 tons). In this way, elastomers were obtained, which could successfully be submitted to the same reprocessing cycle at least two times (Figure 6).

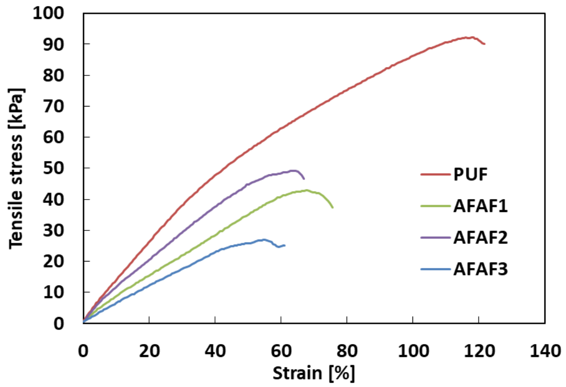

Figure 5. Tensile tests performed on the synthesized foams.

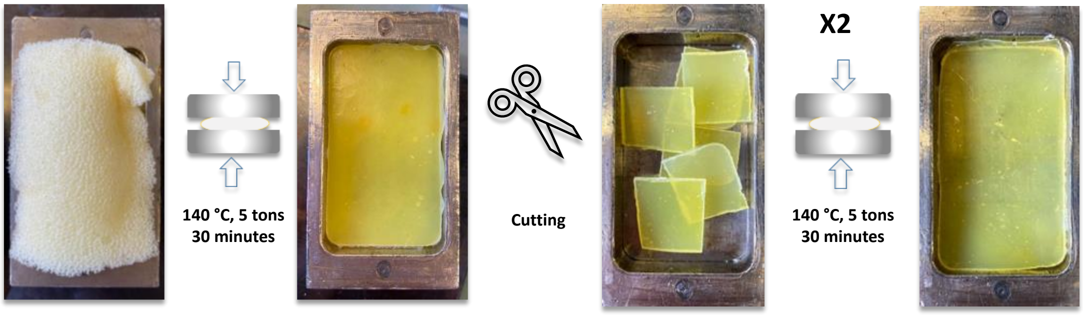

Figure 6. Reprocessing of AFA-based foam into an elastomer, followed by the reprocessing of the obtained elastomer twice.

The required reprocessing temperature for the synthesized foams is considerably higher than for the elastomers, which is ascribed to the formation of permanent bonds during foaming including allophanates, biurets and urea. Solubility tests were conducted on the obtained elastomers to follow any loss of crosslink density. A small increase in soluble fraction was observed after each reprocessing cycle for all synthesized AFAFs (e.g., from 10 to 15% for AFAF2), showing that the elastomers experience a minor loss in crosslink density, which is indicative of a dissociative covalent dynamic network and possible side reactions arising as a result of high catalyst concentrations (Table S3-4). This was further investigated using rheological measurements, where frequency sweeps were performed at 30 °C and the crosslink density was calculated from the obtained storage modulus (G') values at a frequency of 6 Hz (Figure S33, Table S5). On the other hand, no major difference in the T_g-value was noted from the DSC thermograms after each reprocessing cycle (Figure S24). TGA thermograms did not show any significant changes in the $Td_{5\%}$ upon recycling (Figure S26-28) and FTIR spectra did not record any major change, implying that the chemical composition was maintained after three cycles of compression molding (Figure S29). Finally, significant stress relaxation has been observed for all recycled AFAF-materials (R1-version) at temperatures above 120°C, which emphasizes the potential for reprocessing of such foams. In this case, the obtained data were not fitted to a specific model because we expect that the long duration and high temperature rheological analysis (120-160°C) could result in side reactions for such elastomers containing urethane compounds and catalysts, which in turn would affect the stress relaxation behavior (Figure S31). Frequency sweeps performed showed that the material's shear storage modulus slightly decreases with increasing temperature, which confirms again the dissociative behavior of the system (Figure S32).

CONCLUSION

In summary, the dynamic AFA exchange, occurring at temperatures above 80 °C in solvent, has first been investigated in detail with online-FTIR analysis. In the next step, we investigated a large series of catalysts to increase the rate of AFA formation and to make it compatible with the polyurethane foaming process. The use of DBU successfully enhanced the reaction rates, which in turn improved the compatibility with the PU foaming process. The preparation of CANs from acetoacetate-modified polyols and di-isocyanates showed that the chosen approach was efficient on elastomeric level, with no significant loss in material properties after repetitive reprocessing. Moreover, making an elastomeric network that contains both urethane and AFA-bonds showed that it is possible to synthesize a hybrid network while maintaining the dynamic behavior of AFA, which confirmed simultaneously the compatibility of the dynamic chemistry with a PU matrix. Then, the study was pushed to the next level with the synthesis of AFA-based foams. A large series of foams was made in order to finally obtain AFA-based foams that possessed comparable foam properties to standard PUFs, while maintaining dissociative dynamic behavior at elevated temperatures. Instead of incinerating or landfilling PUF, we thus managed to create PUFs with another end-of-life potential. In an upcoming step of the research, it could be envisaged to apply super-critical conditions or other foaming techniques to refoam the obtained elastomers and thus target a foam-to-foam recycling process.

ASSOCIATED CONTENT

The Supporting Information is available free of charge at http://pubs.acs.org showing the synthesis procedure, additional NMR, LCMS, and IR spectra, DSC, and TGA thermograms, stress relaxation data, and foam formulations.

AUTHOR INFORMATION

Corresponding Author

* Filip E. Du Prez, (Polymer Chemistry Research group, Centre of Macromolecular Research (CMaC), Department of Organic and Macromolecular Chemistry, Ghent University, Krijgslaan 281 S4-bis, Ghent B-9000, Belgium; E-Mail: filip.duprez@ugent.be

Present Addresses

†If an author's address is different than the one given in the affiliation line, this information may be included here.

Author Contributions

The manuscript was written through contributions of all authors. All authors have given approval to the final version of the manuscript.

Funding Sources

This project has received funding from the European Union's Horizon 2020 research and innovation program under the Marie Skłodowska-Curie Grant agreement no 860911 (VITRIMAT) and by BOF-UGent (GOA-funding).

Notes

The authors declare no competing financial interest.

ACKNOWLEDGMENT

This project has received funding from the European Union's Horizon 2020 research and innovation program under the Marie Skłodowska-Curie Grant agreement no 860911 (VITRIMAT). F.D.P would also like to thank BOF-UGent for GOA-funding. The authors thank

Bernhard De Meyer and Tom Van Der Snickt for technical support, and Jens Van Hoorde, Dr. Tapas Debsharma, Dr Nezha Badi, Kamil Unal, Irene De Franceschi, and Stephan Maes for the fruitful discussions.

REFERENCES

(1) Polo Fonseca, L.; Duval, A.; Luna, E.; Ximenis, M.; De Meester, S.; Avérous, L.; Sardon, H. Reducing the Carbon Footprint of Polyurethanes by Chemical and Biological Depolymerization: Fact or Fiction? *Curr. Opin. Green Sustain. Chem.* **2023**, *41*, 100802. https://doi.org/10.1016/J.COGSC.2023.100802.

(2) Das, A.; Mahanwar, P. A Brief Discussion on Advances in Polyurethane Applications. *Adv. Ind. Eng. Polym. Res.* **2020**, *3* (3), 93–101. https://doi.org/10.1016/j.aiepr.2020.07.002.

(3) Kemona, A.; Piotrowska, M. Polyurethane Recycling and Disposal: Methods and Prospects. *Polymers (Basel).* **2020**, *12* (8), 1752. https://doi.org/10.3390/POLYM12081752.

(4) Yang, W.; Dong, Q.; Liu, S.; Xie, H.; Liu, L.; Li, J. Recycling and Disposal Methods for Polyurethane Foam Wastes. *Procedia Environ. Sci.* **2012**, *16*, 167–175. https://doi.org/10.1016/J.PROENV.2012.10.023.

(5) Zevenhoven, R. *Treatment and Disposal of Polyurethane Wastes : Options for Recovery and Recycling*; 2004.

(6) Beran, R.; Zarybnicka, | Lucie; Machova, | Dita. Recycling of Rigid Polyurethane Foam: Micro-Milled Powder Used as Active Filler in Polyurethane Adhesives. *J. Appl. Polym. Sci.* **2020**, *137* (37), 49095. https://doi.org/10.1002/app.49095.

(7) Zia, K. M.; Bhatti, H. N.; Ahmad Bhatti, I. Methods for Polyurethane and Polyurethane

Composites, Recycling and Recovery: A Review. *React. Funct. Polym.* **2007**, *67* (8), 675–692. https://doi.org/10.1016/J.REACTFUNCTPOLYM.2007.05.004.

(8) Grdadolnik, M.; Drinčić, A.; Oreški, A.; Onder, O. C.; Utroša, P.; Pahovnik, D.; Žagar, E. Insight into Chemical Recycling of Flexible Polyurethane Foams by Acidolysis. *ACS Sustain. Chem. Eng.* **2022**, *10* (3), 1323–1332. https://doi.org/10.1021/acssuschemeng.1c07911.

(9) Sheel, A.; Pant, D. Chemical Depolymerization of Polyurethane Foams via Glycolysis and Hydrolysis. In *Recycling of Polyurethane Foams*; 2018; pp 67–75. https://doi.org/10.1016/b978-0-323-51133-9.00006-1.

(10) Gama, N.; Godinho, B.; Marques, G.; Silva, R.; Barros-Timmons, A.; Ferreira, A. Recycling of Polyurethane Scraps via Acidolysis. *Chem. Eng. J.* **2020**, *395*. https://doi.org/10.1016/J.CEJ.2020.125102.

(11) Simón, D.; Borreguero, A. M.; De Lucas, A.; Rodríguez, J. F. Glycolysis of Viscoelastic Flexible Polyurethane Foam Wastes. *Polym. Degrad. Stab.* **2015**, *116*, 23–35. https://doi.org/10.1016/J.POLYMDEGRADSTAB.2015.03.008.

(12) Vanbergen, T.; Verlent, I.; De Geeter, J.; Haelterman, B.; Claes, L.; De Vos, D. Recycling of Flexible Polyurethane Foam by Split-Phase Alcoholysis: Identification of Additives and Alcoholyzing Agents to Reach Higher Efficiencies. *ChemSusChem* **2020**, *13* (15), 3835–3843. https://doi.org/10.1002/cssc.202000949.

(13) Deng, Y.; Dewil, R.; Appels, L.; Ansart, R.; Baeyens, J.; Kang, Q. Reviewing the Thermo-Chemical Recycling of Waste Polyurethane Foam. *J. Environ. Manage.* **2021**, *278*, 301–

4797. https://doi.org/10.1016/j.jenvman.2020.111527.

(14) Kloxin, C. J.; Scott, T. F.; Adzima, B. J.; Bowman, C. N. Covalent Adaptable Networks (CANs): A Unique Paradigm in Cross-Linked Polymers. *Macromolecules* **2010**, *43* (6), 2643–2653. https://doi.org/10.1021/ma902596s.

(15) Bowman, C. N.; Kloxin, C. J.; Bowman, [C N; Kloxin, C. J. Covalent Adaptable Networks: Reversible Bond Structures Incorporated in Polymer Networks Angewandte Highlights. *Angew. Chem. Int. Ed* **2012**, *51*, 4272–4274. https://doi.org/10.1002/anie.201200708.

(16) Kloxin, C. J.; Bowman, C. N. Covalent Adaptable Networks: Smart, Reconfigurable and Responsive Network Systems. *Chem. Soc. Rev* **2013**, *42*, 7161. https://doi.org/10.1039/c3cs60046g.

(17) Maes, S.; Scholiers, V.; Du Prez, F. E. Photo-Crosslinking and Reductive Decrosslinking of Polymethacrylate-Based Copolymers Containing 1,2-Dithiolane Rings. *Macromol. Chem. Phys.* **2023**, *224* (1). https://doi.org/10.1002/macp.202100445.

(18) Winne, J. M.; Leibler, L.; Du Prez, F. E. Dynamic Covalent Chemistry in Polymer Networks: A Mechanistic Perspective. *Polym. Chem.* **2019**, *10* (45), 6091–6108. https://doi.org/10.1039/c9py01260e.

(19) Montarnal, D.; Capelot, M.; Tournilhac, F.; Leibler, L. Silica-like Malleable Materials from Permanent Organic Networks. *Science* **2011**, *334* (6058), 965–968. https://doi.org/10.1126/SCIENCE.1212648.

(20) Guerre, M.; Taplan, C.; Winne, J. M.; Du Prez, F. E. Vitrimers: Directing Chemical

Reactivity to Control Material Properties. *Chem. Sci.* **2020**, *11* (19), 4855–4870. https://doi.org/10.1039/d0sc01069c.

(21) Denissen, W.; Winne, J. M.; Du Prez, F. E. Vitrimers: Permanent Organic Networks with Glass-like Fluidity. *Chem. Sci.* **2016**, *7* (1), 30–38. https://doi.org/10.1039/c5sc02223a.

(22) Taplan, C.; Guerre, M.; Du Prez, F. E. Covalent Adaptable Networks Using β-Amino Esters as Thermally Reversible Building Blocks. *J. Am. Chem. Soc.* **2021**, *143* (24), 9140–9150. https://doi.org/10.1021/jacs.1c03316.

(23) Yeh, C. M.; Lin, C. H.; Han, T. Y.; Xiao, Y. T.; Chen, Y. A.; Chou, H. H. Disulfide Bond and Diels-Alder Reaction Bond Hybrid Polymers with High Stretchability, Transparency, Recyclability, and Intrinsic Dual Healability for Skin-like Tactile Sensing. *J. Mater. Chem. A* **2021**, *9* (10), 6109–6116. https://doi.org/10.1039/d0ta10135d.

(24) Fortman, D. J.; Snyder, R. L.; Sheppard, D. T.; Dichtel, W. R. Rapidly Reprocessable Cross-Linked Polyhydroxyurethanes Based on Disulfide Exchange. *ACS Macro Lett.* **2018**, *7* (10), 1226–1231. https://doi.org/10.1021/acsmacrolett.8b00667.

(25) Rekondo, A.; Martin, R.; Ruiz De Luzuriaga, A.; Cabañero, G.; Grande, H. J.; Odriozola, I. Catalyst-Free Room-Temperature Self-Healing Elastomers Based on Aromatic Disulfide Metathesis. *Mater. Horizons* **2014**, *1* (2), 237–240. https://doi.org/10.1039/C3MH00061C.

(26) Zheng, P.; Mccarthy, T. J. A Surprise from 1954: Siloxane Equilibration Is a Simple, Robust, and Obvious Polymer Self-Healing Mechanism. *J. Am. Chem. Soc.* **2012**. https://doi.org/10.1021/ja2113257.

(27) Husted, K. E. L.; Brown, C. M.; Shieh, P.; Kevlishvili, I.; Kristufek, S. L.; Zafar, H.; Accardo, J. V; Cooper, J. C.; Klausen, R. S.; Kulik, H. J.; Moore, J. S.; Sottos, N. R.; Kalow, J. A.; Johnson, J. A. Remolding and Deconstruction of Industrial Thermosets via Carboxylic Acid-Catalyzed Bifunctional Silyl Ether Exchange. *J. Am. Chem. Soc.* **2023**, *145* (3), 1916–1923. https://doi.org/10.1021/jacs.2c11858.

(28) Debsharma, T.; Amfilochiou, V.; Wróblewska, A. A.; De Baere, I.; Van Paepegem, W.; Du Prez, F. E. Fast Dynamic Siloxane Exchange Mechanism for Reshapable Vitrimer Composites. *J. Am. Chem. Soc.* **2022**, *144* (27), 12280–12289. https://doi.org/https://doi.org/10.1021/jacs.2c03518.

(29) Denissen, W.; Droesbeke, M.; Nicola, R.; Leibler, L.; Winne, J. M.; Du Prez, F. E. Chemical Control of the Viscoelastic Properties of Vinylogous Urethane Vitrimers. *Nat. Commun.* **2017**, *8*, 14857. https://doi.org/10.1038/ncomms14857.

(30) Denissen, W.; Rivero, G.; Nicolaÿ, R.; Leibler, L.; Winne, J. M.; Du Prez, F. E. Vinylogous Urethane Vitrimers. *Adv. Funct. Mater.* **2015**, *25* (16), 2451–2457. https://doi.org/10.1002/ADFM.201404553.

(31) Van Lijsebetten, F.; De Bruycker, K.; Spiesschaert, Y.; Winne, J. M.; Du Prez, F. E. Suppressing Creep and Promoting Fast Reprocessing of Vitrimers with Reversibly Trapped Amines. *Angew. Chemie - Int. Ed.* **2022**, *61* (9). https://doi.org/10.1002/anie.202113872.

(32) Spiesschaert, Y.; Guerre, M.; De Baere, I.; Van Paepegem, W.; Winne, J. M.; Du Prez, F. E. Dynamic Curing Agents for Amine-Hardened Epoxy Vitrimers with Short (Re)Processing Times. *Macromolecules* **2020**, *53* (7), 2485–2495.

https://doi.org/https://doi.org/10.1021/acs.macromol.9b02526.

(33) Engelen, S.; Wróblewska, A. A.; De Bruycker, K.; Aksakal, R.; Ladmiral, V.; Caillol, S.; Du Prez, F. E. Sustainable Design of Vanillin-Based Vitrimers Using Vinylogous Urethane Chemistry. *Polym. Chem.* **2022**, *13* (18), 2665–2673. https://doi.org/10.1039/D2PY00351A.

(34) Nishimura, Y.; Chung, J.; Muradyan, H.; Guan, Z. Silyl Ether as a Robust and Thermally Stable Dynamic Covalent Motif for Malleable Polymer Design. *J. Am. Chem. Soc.* **2017**, *139* (42), 14881–14884. https://doi.org/https://doi.org/10.1021/jacs.7b08826.

(35) Van Herck, N.; Maes, D.; Unal, K.; Guerre, M.; Winne, J. M.; Du Prez, F. E. Covalent Adaptable Networks with Tunable Exchange Rates Based on Reversible Thiol–Yne Cross-Linking. *Angew. Chemie Int. Ed.* **2020**, *59* (9), 3609–3617. https://doi.org/10.1002/ANIE.201912902.

(36) Maes, S.; Van Lijsebetten, F.; Winne, J. M.; Du Prez, F. E. N-Sulfonyl Urethanes to Design Polyurethane Networks with Temperature-Controlled Dynamicity. *Macromolecules* **2022**, *56* (5), 1934–1944. https://doi.org/10.1021/acs.macromol.2c02456.

(37) Hernández, A.; Houck, H. A.; Elizalde, F.; Guerre, M.; Sardon, H.; Du Prez, F. E. Internal Catalysis on the Opposite Side of the Fence in Non-Isocyanate Polyurethane Covalent Adaptable Networks. *Eur. Polym. J.* **2022**, *168*, 111100. https://doi.org/10.1016/J.EURPOLYMJ.2022.111100.

(38) Tretbar, C. A.; Neal, J. A.; Guan, Z. Direct Silyl Ether Metathesis for Vitrimers with Exceptional Thermal Stability. *J. Am. Chem. Soc.* **2019**, *141* (42), 16595–16599.

https://doi.org/https://doi.org/10.1021/jacs.9b08876.

(39) Obadia, M. M.; Mudraboyina, B. P.; Serghei, A.; Montarnal, D.; Drockenmuller, E. Reprocessing and Recycling of Highly Cross-Linked Ion-Conducting Networks through Transalkylation Exchanges of C-N Bonds. *J. Am. Chem. Soc.* **2015**, *137* (18), 6078–6083. https://doi.org/https://doi.org/10.1021/jacs.5b02653.

(40) Obadia, M. M.; Jourdain, A.; Cassagnau, P.; Montarnal, D.; Drockenmuller, E. Tuning the Viscosity Profile of Ionic Vitrimers Incorporating 1,2,3-Triazolium Cross-Links. *Adv. Funct. Mater.* **2017**, *27* (45), 1703258. https://doi.org/10.1002/ADFM.201703258.

(41) Guerre, M.; Taplan, C.; Nicolaÿ, R.; Winne, J. M.; Du Prez, F. E. Fluorinated Vitrimer Elastomers with a Dual Temperature Response. *J. Am. Chem. Soc.* **2018**, *140* (41), 13272–13284. https://doi.org/https://doi.org/10.1021/jacs.8b07094.

(42) Taynton, P.; Ni, H.; Zhu, C.; Yu, K.; Loob, S.; Jin, Y.; Qi, H. J.; Zhang, W. Repairable Woven Carbon Fiber Composites with Full Recyclability Enabled by Malleable Polyimine Networks. *Adv. Mater.* **2016**, *28* (15), 2904–2909. https://doi.org/10.1002/adma.201505245.

(43) Jin, K.; Li, L.; Torkelson, J. M.; Jin, K.; Li, L.; Torkelson, M. Recyclable Crosslinked Polymer Networks via One-Step Controlled Radical Polymerization. *Adv. Mater.* **2016**, *28* (31), 6746–6750. https://doi.org/10.1002/ADMA.201600871.

(44) Snyder, R. L.; Fortman, D. J.; De Hoe, G. X.; Hillmyer, M. A.; Dichtel, W. R. Reprocessable Acid-Degradable Polycarbonate Vitrimers. *Macromolecules* **2018**, *51* (2), 389–397. https://doi.org/https://doi.org/10.1021/acs.macromol.7b02299.

(45) Röttger, M.; Domenech, T.; Van Der Weegen, R.; Breuillac, A.; Nicolaÿ, R.; Leibler, L. High-Performance Vitrimers from Commodity Thermoplastics through Dioxaborolane Metathesis. *Science (80-.).* **2017**, *356* (6333), 62–65. https://doi.org/10.1126/science.aah5281.

(46) Quienne, B.; Cuminet, F.; Pinaud, J.; Semsarilar, M.; Cot, D.; Ladmiral, V.; Caillol, S. Upcycling Biobased Polyurethane Foams into Thermosets: Toward the Closing of the Loop. *ACS Sustain. Chem. Eng.* **2022**, *10* (21), 7041–7049. https://doi.org/10.1021/acssuschemeng.2c00950.

(47) Li, J.; Zhu, H.; Fang, D.; Huang, X.; Zhang, C.; Luo, Y. Mechanochemistry Recycling of Polyurethane Foam Using Urethane Exchange Reaction. *J. Environ. Chem. Eng.* **2023**, *11* (3), 110269. https://doi.org/10.1016/j.jece.2023.110269.

(48) Sheppard, D. T.; Jin, K.; Hamachi, L. S.; Dean, W.; Fortman, D. J.; Fortman, D. J.; Ellison, C. J.; Dichtel, W. R. Reprocessing Postconsumer Polyurethane Foam Using Carbamate Exchange Catalysis and Twin-Screw Extrusion. *ACS Cent. Sci.* **2020**, *6* (6), 921–927. https://doi.org/10.1021/ACSCENTSCI.0C00083.

(49) Wang, X. Z.; Lu, M. S.; Zeng, J. B.; Weng, Y.; Li, Y. D. Malleable and Thermally Recyclable Polyurethane Foam. *Green Chem.* **2021**, *23* (1), 307–313. https://doi.org/10.1039/d0gc03471a.

(50) Houbben, M.; Thomassin, J.-M.; Jé Rô Me, C. Supercritical CO 2 Blown Poly(e-Caprolactone) Covalent Adaptable Networks towards Unprecedented Low Density Shape Memory Foams †. *Cite this Mater. Adv* **2022**, *3*, 2918. https://doi.org/10.1039/d2ma00040g.

(51) Lan, B.; Li, P.; Yang, Q.; Gong, P. Dynamic Self Generation of Hydrogen Bonding and Relaxation of Polymer Chain Segment in Stabilizing Thermoplastic Polyurethane Microcellular Foams. *Mater. Today Commun.* **2020**, *24*, 101056. https://doi.org/10.1016/J.MTCOMM.2020.101056.

(52) Chen, Y. H.; Cheng, Y. C.; Rwei, S. P. Bio-Based Poly(Imine-Amide) Materials with Dynamic Covalent Adaptable Networks: Toward Conductive Composites and Thermally Moldable Microcellular Foams. *ACS Sustain. Chem. Eng.* **2022**, *10* (45), 14794–14805. https://doi.org/https://doi.org/10.1021/acssuschemeng.2c04183.

(53) Liu, Y. B.; Peng, L. M.; Bao, R. Y.; Yang, M. B.; Yang, W. Vitrimeric Polylactide by Two-Step Alcoholysis and Transesterification during Reactive Processing for Enhanced Melt Strength. *ACS Appl. Mater. Interfaces* **2022**, *14* (40), 45966–45977. https://doi.org/https://doi.org/10.1021/acsami.2c15595.

(54) Belmonte, P.; Ramos, M. J.; Rodríguez, J. F.; García, M. T.; Imbernon, L.; García-Vargas, J. M. Reprocessing of Thermoset Polythiourethanes into Foams Using Supercritical CO2. *J. Supercrit. Fluids* **2023**, *199* (March), 105972. https://doi.org/10.1016/j.supflu.2023.105972.

(55) Wicks, Z. W.; Wu, K. J. Reactions of Acetoacetic Ester Blocked Cyclohexyl Isocyanate. *J. Org. Chem.* **1980**, *45* (12), 2446–2448. https://doi.org/https://doi.org/10.1021/jo01300a036.

(56) Zhu, Y.; Gao, F.; Wei, X.; Cheng, Q.; Zhao, J.; Cao, Z.; Cao, J.; Zhong, J.; Lin, C.; Shu, J.; Shen, L. A Novel Bio-Based Coating Material Prepared from Modified Acetoacetylated Castor Oil and Diisocyanate. *Prog. Org. Coatings* **2020**, *138*, 105397.

https://doi.org/10.1016/J.PORGCOAT.2019.105397.

(57) Narayan, R.; Chattopadhyay, D. K.; Sreedhar, B.; Raju, K. V. S. N.; Mallikarjuna, N. N.; Aminabhavi, T. M. Degradation Profiles of Polyester-Urethane (HP-MDI) and Polyester-Melamine (HP-HMMM) Coatings: A Thermal Study. *J. Appl. Polym. Sci.* **2005**, *97* (2), 518–526. https://doi.org/10.1002/APP.21770.

(58) Vogt-Birnbrich, B. Novel Synthesis of Low VOC Polymeric Dispersions and Their Application in Waterborne Coatings. *Prog. Org. Coatings* **1996**, *29* (1–4), 31–38. https://doi.org/10.1016/S0300-9440(96)00627-3.

(59) Liu, Z.; Yu, C.; Zhang, C.; Shi, Z.; Yin, J. Revisiting Acetoacetyl Chemistry to Build Malleable Cross-Linked Polymer Networks via Transamidation. *ACS Macro Lett.* **2019**, *8* (3), 233–238. https://doi.org/10.1021/acsmacrolett.9b00010.

(60) Ma, Y.; Liu, Z.; Zhou, S.; Jiang, X.; Shi, Z.; Yin, J. Aminoesterenamide Achieved by Three-Component Reaction Heading toward Tailoring Covalent Adaptable Network with Great Freedom. *Macromol. Rapid Commun.* **2021**, *42* (20). https://doi.org/10.1002/marc.202100394.

(61) Bai, J.; Shi, Z. Macromolecular Metabolism Based on Enaminoneamide Achieving Transformation of Polymer Architecture. *Chem. Mater.* **2022**, *34* (13), 6026–6035. https://doi.org/10.1021/acs.chemmater.2c01129.

(62) Nasar, A. S.; Libni, G. Forward and Reverse Reactions of N-Methylaniline-Blocked Polyisocyanates: A Clear Step into Double Arrhenius Plots and Equilibrium Temperature of Thermally Reversible Reactions. *RSC Adv.* **2017**, *7* (54), 34149–34159.

https://doi.org/10.1039/c7ra03734a.

(63) Ji, Y.; Yang, X.; Ji, Z.; Zhu, L.; Ma, N.; Chen, D.; Jia, X.; Tang, J.; Cao, Y. DFT-Calculated IR Spectrum Amide I, II, and III Band Contributions of N-Methylacetamide Fine Components. *ACS Omega* **2020**, *5* (15), 8572–8578. https://doi.org/https://doi.org/10.1021/acsomega.9b04421.

(64) Bakkali-Hassani, C.; Berne, D.; Ladmiral, V.; Caillol, S. Transcarbamoylation in Polyurethanes: Underestimated Exchange Reactions? *Macromolecules* **2022**, *55* (18), 7974–7991. https://doi.org/10.1021/acs.macromol.2c01184.

(65) Elizalde, F.; Aguirresarobe, R. H.; Gonzalez, A.; Sardon, H. Dynamic Polyurethane Thermosets: Tuning Associative/Dissociative Behavior by Catalyst Selection. *Polym. Chem.* **2020**, *11* (33), 5386–5396. https://doi.org/10.1039/d0py00842g.

(66) Chen, X.; Hu, S.; Li, L.; M. Torkelson, J. Dynamic Covalent Polyurethane Networks with Excellent Property and Cross-Link Density Recovery after Recycling and Potential for Monomer Recovery. *ACS Appl. Polym. Mater.* **2020**, *2* (5), 2093–2101. https://doi.org/10.1021/acsapm.0c00378.

(67) Bloodworth, A. J.; Davies, A. G. 975. Organometallic Reactions. Part I. The Addition of Tin Alkoxides to Isocyanates. *J. Chem. Soc.* **1965**, No. 0, 5238–5244. https://doi.org/10.1039/JR9650005238.

(68) Sardon, H.; Pascual, A.; Mecerreyes, D.; Taton, D.; Cramail, H.; Hedrick, J. L. Synthesis of Polyurethanes Using Organocatalysis: A Perspective. *Macromolecules* **2015**, *48* (10), 3153–3165. https://doi.org/10.1021/acs.macromol.5b00384.

TOC